DMD Fast Forward. Published on March 10, 2017 as DOI: 10.1124/dmd.117.075200
This article has not been copyedited and formatted. The final version may differ from this version.

DMD # 75200

Phase II Conjugates of Urolithins Isolated from Human Urine and Potential Role of *β*-glucuronidases in Their Disposition

Jakub P. Piwowarski, Iwona Stanisławska, Sebastian Granica, Joanna Stefańska, and Anna K. Kiss

Department of Pharmacognosy and Molecular Basis of Phytotherapy, Medical University of Warsaw, Faculty of Pharmacy (J.P.P., I.S., S.G., A.K.K.); Department of Pharmaceutical Microbiology, CePT, Medical University of Warsaw (J.S.)

Primary Laboratory of Origin: Medical University of Warsaw, Faculty of Pharmacy

DMD Fast Forward. Published on March 10, 2017 as DOI: 10.1124/dmd.117.075200
This article has not been copyedited and formatted. The final version may differ from this version.

Running Title: Urolithin conjugates. *β*-glucuronidases and disposition.

Address correspondence to:

Dr. Jakub Piwowarski

Department of Pharmacognosy and Molecular Basis of Phytotherapy

Medical University of Warsaw

Faculty of Pharmacy

Banacha 1

02-097 Warsaw

Poland

Phone: +48 22 5720953

Fax: +48 22 5720942

E-mail: jakub.piwowarski@wum.edu.pl

Number of Text Pages: 30

Number of Tables: 1

Number of Figures: 7

Number of References: 48

Number of Words in Abstract: 250

Number of Words in Introduction: 545

Number of Words in Discussion: 1500

DMD Fast Forward. Published on March 10, 2017 as DOI: 10.1124/dmd.117.075200
This article has not been copyedited and formatted. The final version may differ from this version.

List of Non-Standard Abbreviations:

ETs	ellagitannins
UA	urolithin A
iUA	iso-urolithin A
UB	urolithin B
GiUA	iso-urolithin A glucuronide
GUA	urolithin A glucuronide
GUB	urolithin B glucuronide
GSUA	urolithin A sulfate-glucuronide
f-MLP	N-Formylmethionine-leucyl-phenylalanine
FPR1	formyl peptide receptor-1
MUG	4-methylumbelliferyl-β-D-glucuronide

DMD Fast Forward. Published on March 10, 2017 as DOI: 10.1124/dmd.117.075200
This article has not been copyedited and formatted. The final version may differ from this version.

ABSTRACT

In recent years, many xenobiotics derived from natural products have been shown to undergo extensive metabolism by gut microbiota. Ellagitannins, which are high molecular polyphenols, are metabolized to dibenzo[*b*,*d*]pyran-6-one derivatives-urolithins. These compounds, in contrast with their parental compounds, have good bioavailability and are found in plasma and urine at micromolar concentrations. *In vivo* studies conducted for ellagitannin-containing natural products indicate their beneficial health effects towards inflammation and cancer, which are associated with the formation of urolithins. However, the great majority of *in vitro* experiments that have revealed the molecular mechanisms responsible for the observed effects were conducted for urolithin aglycones. These studies are thus incongruent with the results of pharmacokinetic studies that clearly indicate that glucuronide conjugates are the dominant metabolites present in plasma, tissue and urine. The aim of this study was to isolate and structurally characterize urolithin conjugates from the urine of a volunteer who ingested ellagitannin-rich natural products and to evaluate the potential role of *β*-glucuronidases-triggered cleavage in urolithin disposition. Glucuronides of urolithin A, iso-urolithin A and urolithin B were isolated and shown to be cleaved by the *β*-glucuronidases released by neutrophils from azurophilic granules upon f-MLP stimulation as well as by *E. coli* standard strains and clinical isolates from patients with urinary tract infections. These results justify the hypothesis that the selective activation of urolithin glucuronides by *β*-glucuronidase, which are present at high concentrations at inflammation and infection sites and in the microenvironments of solid tumors, could locally increase the concentration of bioactive urolithin aglycones.

DMD Fast Forward. Published on March 10, 2017 as DOI: 10.1124/dmd.117.075200
This article has not been copyedited and formatted. The final version may differ from this version.

Introduction

Accumulating evidence has revealed the diverse effects of the gut microbiota on human health, including nutrition, physiology and host metabolism. In recent years, the metabolic crosstalk between a host and its gut microbiota in modulating the pharmacokinetics and pharmacodynamics of drugs has gained much attention (Klaassen and Cui, 2015; Yip and Chan, 2015). Many xenobiotics derived from food products and medicinal plant materials have been shown to undergo extensive metabolism by gut microbiota, resulting in the formation of small molecular metabolites that not only are more bioavailable than parental compounds but also reveal interesting pharmacological properties (Kieran and Del Rio, 2015). One of the most widely studied gut microbiota metabolites of natural products are the urolithins. These 6*H*-dibenzo[*b*,*d*]pyran-6-one derivatives are produced by gut microbiota from high-molecular-weight polyphenols, namely, the ellagitannins (ETs), which are constituents of various medicinal plants and food products. In contrast with parental ETs, urolithins have good bioavailability and are found in plasma and urine at micromolar concentrations. After absorption, urolithins rapidly undergo Phase II metabolism, resulting in their presence in plasma and tissues mostly in a conjugated form; these metabolites are mainly glucuronides and, to a lesser extent, sulfates. After absorption in the gut, only traces of non-conjugated compounds were detected in bodily fluids, indicating that conjugation has already taken place in the gut epithelium (Gonzalez-Barrio et al., 2010; Gonzalez-Sarrias et al., 2014; Nunez-Sanchez et al., 2014; Mora-Cubillos et al., 2015; Garcia-Villalba et al., 2016; Tomas-Barberan et al., 2016).

In vivo and clinical studies conducted for ET-containing natural products clearly indicate beneficial health effects, especially towards inflammation-associated

DMD Fast Forward. Published on March 10, 2017 as DOI: 10.1124/dmd.117.075200
This article has not been copyedited and formatted. The final version may differ from this version.

diseases and cancer, which are often connected with the formation and absorption of urolithins within the gut (Larrosa et al., 2010a; Larrosa et al., 2010b; Espin et al., 2013; Tomas-Barberan et al., 2016). These results are accompanied by *in vitro* studies for urolithins that unambiguously confirm their anti-inflammatory and anti-proliferative activities and reveal the molecular mechanisms that are potentially responsible for the observed effects (Gonzalez-Sarrias et al., 2009; Piwowarski et al., 2014a; Piwowarski et al., 2015; Gonzalez-Sarrias et al., 2016).

One important issue that has recently been raised is the inconsistency of *in vitro* bioactivity results compared with *in vivo* and clinical pharmacokinetic studies. The great majority of *in vitro* experiments were conducted for urolithin aglycones, making them incongruent with the results of pharmacokinetic studies that clearly indicate that glucuronide conjugates of urolithins are the dominant metabolites present in plasma, tissues and urine (Tomas-Barberan et al., 2016).

Although urolithin glucuronides are the main metabolites detected in bodily fluids, the highly enzymatically active environment of inflammation and cancer sites should be considered, as they have the potential to trigger structural alterations. One of the most common, abundant enzymes at these sites is *β*-glucuronidase, which is released from infiltrating inflammatory cells and the lysosomes of necrotic cells (Tranoy-Opalinski et al., 2014). *β*-glucuronidase is also a characteristic enzyme of *Escherichia coli*, the bacterial species that is responsible for urinary tract infections, among other disease (Chang et al., 1989).

The aim of the study was to isolate and structurally characterize the urolithin conjugates from the urine of a volunteer after ingestion of ET-rich natural products and to evaluate whether they undergo cleavage under the influence of *β*-glucuronidases released by human neutrophils, as well as by various *E. coli* strains.

DMD Fast Forward. Published on March 10, 2017 as DOI: 10.1124/dmd.117.075200
This article has not been copyedited and formatted. The final version may differ from this version.

Materials and Methods

Reference Compounds and Chemicals

Standards of urolithin A (UA), iso-urolithin A (iUA), urolithin B (UB) and urolithin C (UC) were isolated from human gut microbiota cultures using a previously described method (Piwowarski et al., 2016). The purity of examined compounds (≥95%) was confirmed using a UHPLC-DAD-MS^n method. *Lythrum salicaria* herb aqueous extract was prepared as described previously (Piwowarski and Kiss, 2013). The chromatogram obtained with UHPLC-DAD-MS^n method presenting its ellagitannin profile is provided in Supplemental Data Figure S2.

Subject and Dosing Procedure

We chose a healthy volunteer (male, aged 30) based on our previous study, which identified the volunteer as possessing microbiota that produce the most diverse pattern of urolithins (Piwowarski et al., 2016). The volunteer was asked to supplement his diet with products rich in ETs. Pomegranate juice (0.5 L/day), walnuts (30 g/day), hazelnuts (30 g/day) and fresh raspberries (200 g/day) were consumed for five days. The total urine was collected from day 1 to day 5 and stored at -20 °C in a total combined volume of 5.5 L of urine. The study respected the 1964 Declaration of Helsinki for the ethical treatment of human subjects for biomedical research.

UHPLC Analysis of Urine

An SPE Chromabond C_{18} Hydra column (Macherey-Nagel, Germany) was preconditioned with 10 mL of MeOH and 10 mL of H_2O. Fifteen mL of urine was applied to the column and washed with 10 mL of H_2O before elution with 2 mL of MeOH. The eluate was subjected to UHPLC-DAD-MS^n analysis.

DMD Fast Forward. Published on March 10, 2017 as DOI: 10.1124/dmd.117.075200
This article has not been copyedited and formatted. The final version may differ from this version.

Isolation of Metabolites and Structure Determination

Urine (5.5 L) was concentrated under reduced pressure at 40 °C to 3.0 L and extracted four times with 2 L of EtOAc. The aqueous residue (3.0 L) was subjected to Diaion HP-20 (Supelco) column (40 cm × 5 cm) chromatography and subsequently eluted with 3.0 L of H_2O, 20% MeOH and 100% MeOH. The fraction eluted with 100% MeOH (3.7 g) was chromatographed on a silica gel 60 column (27 cm × 3 cm) eluted with MeOH - $CHCl_3$ (0:100 → 100:0 *v/v* in 7 steps) to give 104 fractions pooled into 11 main fractions C_1 – C_{11}. Fraction C_5 (543 mg) was purified using a preparative HPLC system (Shimadzu LC20-AP instrument, Japan, Zorbax SB-C_{18} 150 mm × 21.2 mm × 5.0 μm, λ_1=254 nm, λ_2=350 nm, flow 9 mL/min, mobile phase: 0.1% HCOOH in water (A) and 0.1% HCOOH in MeCN (B), elution program: 10 – 40% B; 0-40 min) to give urolithin B glucuronide (**GUB**) (23.80-24.40 min; 25 mg) and UB (31.5-32.0 min; 8 mg). Fractions C_8 (244 mg) and C_9 (37 mg) were chromatographed on a Sephadex LH-20 column (137 cm × 2 cm) and eluted with mixture of MeOH:water (1:1, *v/v*) to obtain 140 fractions pooled into 9 fractions D_1 – D_9. Fractions D_3 (54 mg) and D_4 (16 mg) were combined and subjected to a preparative HPLC system (elution program: 15 – 20% B; 0-40 min) to give urolithin A glucuronide (**GUA**) (10.05-12.65 min; 31 mg), iso-urolithin A glucuronide (**GiUA**) (13.00-14.50 min; 6 mg) and urolithin B glucuronide (**GUB**) (31.60-33.80 min; 4 mg). Fraction C_7 (1159 mg) was chromatographed on a Sephadex LH-20 column (MeOH:water, 1:1, *v/v*) to give 297 fractions pooled into 17 fractions E_1 – E_{17}. Fraction E_5 (362 mg) was subjected to a preparative HPLC system (parameters same as for fraction D_3+D_4) to obtain **GUA** (10.4-12.55 min; 94 mg), **GiUA** (12.56-14.5 min; 14 mg) and **GUB** (31.60-33.80 min; 44 mg). Fractions D_2 (22 mg) and E_4 (141 mg) were combined and subjected to a preparative HPLC system (parameters same as for fraction C_5) to give **GUB** (23.70-

DMD Fast Forward. Published on March 10, 2017 as DOI: 10.1124/dmd.117.075200
This article has not been copyedited and formatted. The final version may differ from this version.

24.50 min; 21 mg). Fraction C_6 (811 mg) was chromatographed on a Sephadex LH-20 column (MeOH:water, 1:1, *v/v*) to give 241 fractions pooled into 18 fractions F_1 – F_{18}. Fractions F_{11} (75 mg) and F_{12} (46 mg) were combined and subjected to a preparative HPLC system (as for fraction C_5) to obtain **GUB** (23.60-24.10 min; 45 mg) and UB (31.00-31.70 min; 6 mg).

The EtOAc fraction (2.8 g) was chromatographed on a silica gel 60 (Machery-Nagel, Duren, Germany) column (27 cm × 3 cm) eluted with MeOH - $CHCl_3$ (0:100 → 100:0 v/v in 9 steps) to give 140 fractions pooled into 10 main fractions A_1 – A_{10}. Fractions A_2+A_3 (91.7 mg) contained UB as the major compound, which was purified using preparative HPLC (31.50-32.00 min, 4 mg).

^{1}H and ^{13}C NMR spectra were recorded at 25 °C on a VARIAN VNMRS instrument (300 MHz for ^{1}H and 75 MHz for ^{13}C NMR). DMSO-d_6 was used as a solvent. Chemical shifts (δ) are reported in ppm, and coupling constants (*J*) are reported in Hz. The assignments were based on HSQC and HMBC experiments.

Gut microbiota *ex vivo* metabolism

Evaluation of the *ex vivo* metabolism of ellagitannins by the volunteer's gut microbiota was performed as described previously (Piwowarski et al., 2014b). To acquire anaerobic conditions, a brain heart infusion (BHI), (DIFCO, Detroit, MI, USA) was boiled and immediately cooled before the experiment. Forty mg of *Lythrum salicaria* L. extract (phytochemically standardized ET source) was dissolved in 1 mL of distilled water and sterilized by filtration through an Ophtalsart hydrophilic syringe filter (0.2 mm) (Sartorius Stedim Biotech GmbH, Germany). One mL of 10% fecal slurry in BHI and 0.5 mL of extract solution were added to 8.5 mL of BHI. The batch cultures were incubated in a sealed container under anaerobic conditions using GENbox anaer sachets (bioMerieux, France) at 37 °C. After 24 h, the batch culture

DMD Fast Forward. Published on March 10, 2017 as DOI: 10.1124/dmd.117.075200
This article has not been copyedited and formatted. The final version may differ from this version.

was extracted three times with 10 mL of diethyl ether. The organic layers were evaporated to dryness and re-dissolved in 500 μL of MeOH for UHPLC-DAD-MS^n analysis.

Neutrophils Isolation

Peripheral venous blood was taken from four healthy human donors (males, 20-35 years old) at the Warsaw Blood Donation Centre. Donors did not smoke or take any medication. They were clinically confirmed to be healthy, and routine laboratory tests showed values within the normal range. The study conformed to the principles of the Declaration of Helsinki. Neutrophils were isolated with a standard method of dextran sedimentation and subsequent hypotonic lysis of erythrocytes and centrifugation in a Ficoll Hypaque gradient (Piwowarski et al., 2014a). The purity of neutrophils was >97%, and viability as measured by trypan blue exclusion was >98%.

Deglucuronidation assay: After isolation, neutrophils were resuspended in HBSS (6×10^5 cells/mL) primed with cytochalasin B (5 μg/mL) for 5 min and stimulated with f-MLP (1 μM) for 10 min. The neutrophils were centrifuged (2,000 rpm; 10 min; 4 °C). The supernatant was acidified with lactic acid to pH=5.2 and incubated with **GiUA**, **GUA** and **GUB** at a final concentration of 50 μM. After 24 h, 300 μL reaction mixture was mixed with 400 μL MeOH, subjected to an ultrasonication for 5 min and centrifuged (14000 g, 10 min). The hydrolysis of glucuronides was monitored using a UHPLC-DAD-MS^n method. The amount of released *β*-glucuronidase in supernatants was determined using a human *β*-glucuronidase ELISA Kit (Wuhan Fine Biological Technology Co., Ltd, Wuhan, China) according to the manufacturer's instructions.

DMD Fast Forward. Published on March 10, 2017 as DOI: 10.1124/dmd.117.075200
This article has not been copyedited and formatted. The final version may differ from this version.

Deglucuronidation in *E. coli in vitro* cultures

E. coli NCTC 10538, ATCC 25922 strains and clinical isolates (C1- C7) were streaked over a Trypticase Soy Agar plate (Becton Dickinson) and incubated for 24 h at 37 °C. A single colony was used to inoculate 10 mL of BHI, which was incubated for 24 h at 37 °C. To 240 µL of culture, 60 µL of the respective glucuronide solution in PBS was added (final concentration of glucuronide: 50 µM) and incubated for 24 h at 37 °C. Next, 400 µL of MeOH was added to 250 µL of culture, subjected to ultrasonication and centrifuged (14000 g, 10 min). The hydrolysis of glucuronides was monitored using a UHPLC-DAD-MS^n method.

Chromatographic methods

UHPLC-DAD-MS^n analyses were performed using a UHPLC-3000 RS system (Dionex, Germany) with DAD detection and an AmaZon SL mass spectrometer with the ESI interface (Bruker Daltonik GmbH, Germany). A Zorbax SB-C_{18} (150 mm x 2.1 mm x 1.9 µm) (Agilent, USA) column was used. The mobile phase consisted of 0.1% HCOOH in water (A) and 0.1% HCOOH in MeCN (B). The gradient was: 0–5 min 0% B, 5–15 min 0–10% B, 15–25 min 10–20% B and 25–35 min 20–30% B, 35–45 min 30–50% B, 45–50 min 50–100% B and 50–60 min 100% B. The column temperature was maintained at 25 °C, and the flow rate was 0.200 mL/min. The LC eluate was introduced into the ESI interface without splitting, and compounds were analyzed in the negative and positive ion modes with the following settings: nebulizer pressure of 40 psi; drying gas flow rate of 9 L/min; nitrogen gas temperature of 300 °C; and capillary voltage of 4.5 kV. The mass scan ranged from 100 to 2200 *m/z*. UV spectra were recorded from 200–400 nm. The presence of UA, iUA, UB and UC was confirmed by comparing retention times and UV and *m/z* spectra with authentic

DMD Fast Forward. Published on March 10, 2017 as DOI: 10.1124/dmd.117.075200
This article has not been copyedited and formatted. The final version may differ from this version.

samples. Other compounds were tentatively assigned based on their chromatographic properties, namely, UV and MS spectra.

Statistical analysis

The results are shown as the mean values ± SEM. The statistical significance of differences between means was determined by one-way ANOVA. For comparison of results between the groups, Tukey's *post hoc* test was used. Results with p-value < 0.05 were considered statistically significant. All analyses were performed using Statistica 10 software.

Results

Profile of urinary metabolites. UHPLC-DAD-MS/MS analysis has shown that the regular weekly intake of ET-rich products results in secretion of Phase II conjugates of urolithins in urine (Fig. 2A). Metabolites were identified based on their retention times and UV and MS/MS data. The major metabolite was **GUA**, which gave a pseudomolecular ion at *m/z* = 403 and an ion fragment at 227 representing a neutral loss of 176 amu that is characteristic of glucuronic acid. **GiUA,** with a similar pseudomolecular ion and fragmentation pattern, was distinguished from **GUA** based on UV spectra (Gonzalez-Barrio et al., 2011). **GUB** gave a pseudomolecular ion at *m/z* = 387 and a fragment ion at 211. Small amounts of urolithin A sulfate-glucuronide (GSUA) were detected at *m/z* = 483 and the MS^2 ion at 307 (neutral loss of 176 amu) which fragmented to 227 (characteristic for neutral sulfate loss of 80 amu). Apart from Phase II conjugates, small amounts of iUA, UA and UB were also detected.

Metabolite isolation and structural determination. By means of liquid-liquid extraction, column chromatography and preparative high-performance liquid

DMD Fast Forward. Published on March 10, 2017 as DOI: 10.1124/dmd.117.075200
This article has not been copyedited and formatted. The final version may differ from this version.

chromatography, three major glucuronide metabolites were isolated from human urine—**GiUA**, **GUA**, **GUB** (Fig. 1)—as was UB. The structures were determined using ^{1}H, ^{13}C NMR, HSQC and HMBC spectra (Table 1). All metabolites were identified as *β*-anomers based on the anomeric H-1 signal appearing at δ 5.0 as a doublet, with a coupling constant near 7 Hz (Pearson et al., 2005). The downfield shift of H2 and H4 in the **GiUA** spectrum, compared to to its aglycone (Piwowarski et al., 2016), indicates glucuronidation of the OH group at C3. The analogous shifts were observed for H2 and H4 of urolithin A 3-*O*-glucuronide and H7 and H9 of urolithin A 8-*O*-glucuronide. The total amounts of obtained compounds were 20 mg of **GiUA**, 125 mg of **GUA**, 139 mg of **GUB** and 18 mg of **UB**. **GUA** was isolated as a mixture of urolithin A-3-*O*-glucuronide and urolithin A-8-*O*-glucuronide as revealed by NMR spectra, which have shown two sets of proton (Fig. 3) and carbon signals. It was impossible to separate these two isomers using available chromatographic methods. However, complete proton and carbon assignments were performed based on 2D NMR spectra (Table 1).

Gut microbiota *ex vivo* metabolism. In all, iUA, UA, UB, and UC were determined in the volunteer's gut microbiota cultures (Fig. 2B). Their identities were confirmed by comparison of retention times, UV and MS data with standard substances. The most abundant peak was observed for iUA, while only small amounts of UA were detected.

Deglucuronidation by human neutrophils. Neutrophils isolated from human peripheral venous blood were primed with cytochalasin B and subsequently stimulated with f-MLP to release the azurophilic granules containing *β*-glucuronidase. The supernatant pH was adjusted to 5.2 – which is known to be an optimal value for

DMD Fast Forward. Published on March 10, 2017 as DOI: 10.1124/dmd.117.075200
This article has not been copyedited and formatted. The final version may differ from this version.

enzyme activity (Ho, 1985). Incubation of **GiUA**, **GUA** and **GUB** with supernatants resulted in enzymatic cleavage of β-glycosidic bonds and release of the respective aglycones (Fig. 4A and 5). The deglucuronidation process was significantly enhanced when neutrophils were stimulated with cytochalasin B and f-MLP in comparison to untreated cells. When pH was adjusted beyond the optimal values (pH=7.2 in the case of HBSS without lactic acid and pH=3.5 when excessive acidification was applied), deglucuronidation was not observed (data not shown). To evaluate whether *β*-glucuronidase is responsible for the cleavage, its concentration was determined using an ELISA test. Significantly higher enzyme protein concentrations in supernatants were observed upon stimulation. In addition, differences in the amounts of f-MLP-triggered enzyme release were observed between blood donors (D1-D4) that were strictly correlated with the extent of deglucuronidation (Fig. 4B). No significant differences in the compounds' susceptibility to enzymatic cleavage were observed.

Deglucuronidation in *E. coli* cultures. Two reference *E. coli* strains, NCTC 10538 and ATCC 25922, and 7 clinical isolates (C1-C7) obtained from patients suffering from urinary tract infections were used for examinations. Cultures in Fluorocult VRB Agar plates (Merck) revealed that the strains expressed different abilities to hydrolyze 4-methylumbelliferyl-*β*-D-glucuronide (MUG) (Fig. 6). The most intense blue fluorescence from free 4-methylumbelliferone was observed in the *E. coli* C1 strain, while *E. coli* NCTC 10538 and C6 showed no fluorescence. Incubation of **GiUA**, **GUA** and **GUB** with selected *E. coli* strains and isolates resulted in deglucuronidation and release of the respective aglycones (Fig. 7, Supplemental Data Figure S1). No hydrolysis was observed when compounds were incubated in BHI medium without bacteria inoculation. The most active strain was C1, which was

DMD Fast Forward. Published on March 10, 2017 as DOI: 10.1124/dmd.117.075200
This article has not been copyedited and formatted. The final version may differ from this version.

also the most potent in MUG cleavage. The non-MUG-degrading *E. coli* isolate C6 only hydrolyzed the tested glucuronides to a small extent. Comparison of cleavage rates for each glucuronide revealed that in the case of clinical isolates, **GUB** was the most susceptible for degradation.

Discussion

The chosen volunteer was assigned as metabotype B (producing iUA, UA, and UB) (Tomas-Barberan et al., 2014). In addition to Phase II metabolites, the respective aglycones were also detected in urine. They were not only found when total collected urine was analyzed (Fig. 2A) but also when samples were analyzed immediately after collection (data not shown), which excludes the possibility of their formation through storage-triggered hydrolysis. The most abundant metabolite was **GUA**, while *ex vivo* cultures of the volunteer's gut microbiota showed the reverse pattern, with significant dominance of iUA. This observed iUA dominance was in concordance with previous studies conducted on single ETs using the volunteer's gut microbiota (see volunteer D3 in our previous paper Piwowarski et al., 2016). This discrepancy could be explained by different metabolic activity in gut microbiota *in vivo* and *ex vivo* or by differences in the metabolic and/or elimination pathways between UA and iUA. Although the volunteer's microbiota were able to produce UC, no phase II metabolites of this compound were detected in urine.

Phase II metabolites of urolithins were isolated from human urine and their structures were fully described based on the NMR spectra. NMR data for **GUA** and **GUB** were in concordance with ^{1}H spectra for compounds obtained through chemical synthesis (Lucas et al., 2009; Gonzalez-Sarrias et al., 2013). The 1D and 2D NMR spectra allowed full assignment of the ^{1}H and ^{13}C signals for the first time. The

DMD Fast Forward. Published on March 10, 2017 as DOI: 10.1124/dmd.117.075200
This article has not been copyedited and formatted. The final version may differ from this version.

formation of two **GUA** regioisomers, i.e., urolithin A 3-*O*-glucuronide and urolithin A-8-*O*-glucuronide, was thus fully confirmed *in vivo*. As in previously described methods for **GUA** biosynthesis, we were unable to separate the two **GUA** isomers (Gimenez-Bastida et al., 2012), because they co-eluted in the applied column chromatography resins and the analytical RP18 UHPLC column. However, using 2D NMR experiments, we were able to distinguish two series of signals. Based on comparison of their intensities, it can be postulated that glucuronidation at position 8 is favorable. In the future, methods to separate these compounds should be developed. However, this mixture can still be used in bioassays, as it potentially reflects the actual proportion of these metabolites in bodily fluids. The identification presented here is in concordance with previous studies using HPLC-TOFMS-SPE-NMR analysis of urine from patients who ingested tea (van der Hooft et al., 2012). For the first time **GiUA**, which was found only as the 3-*O*-glucuronide, was isolated from human urine. The developed method yields significant amounts of Phase II metabolites of urolithins, which can be then applied to evaluate the *in vivo* effects and mechanisms of ET microbiota metabolites. The isolation of **GiUA** is of particular importance, as 10-50% of population has been identified as **iUA** producers (Tomas-Barberan et al., 2014). This compound has not previously been synthesized or isolated from biological fluids.

The concentration of Phase II urolithin metabolites in human plasma and urine can reach 35 μM and 100 μM respectively, while aglycones are present in significantly lower concentrations – 0.005 μM and 10 μM respectively (Tomas-Barberan et al., 2016). In prostate and colon tissues urolithin glucuronides were found at nanomolar concentrations (Gonzalez-Sarrias et al., 2010). Both the aglycones and their conjugates ranged from 4.8 and 507.3 ng/g in human colon

tissue samples (Nunez-Sanchez et al., 2014). The administration of UA to rats showed that the distribution of this compound and its conjugated metabolites among different organs reached concentrations up to 1050 ng/g (Seeram et al., 2007).

Although urolithin conjugates were clearly shown to dominate in plasma, tissues and urine following the administration of ET-rich natural products, the majority of *in vitro* studies have focused on non-conjugated molecules. Only a few studies investigate urolithin Phase II metabolites, the majority of which have shown significant *in vitro* and *in silico* decreases in activity for conjugated compounds. The Phase-II metabolism of urolithins in different cell lines is considered a mechanism of cancer cells resistance against urolithins, due to their conversion to glucuronide conjugates, which were shown to exert significantly lower anti-proliferative activity (Adams et al., 2010; Dellafiora et al., 2013; Gonzalez-Sarrias et al., 2014; Gonzalez-Sarrias et al., 2015; Larrosa et al., 2006; Sala et al., 2015). This is the first report of a reversed process of deglucuronidation. Differences in anti-inflammatory activity between **GUA** and UA were only shown by Gimenez-Bastida et al., 2012, while urolithin methylation was shown to lead to significant activity loss or decrease (Piwowarski et al., 2014a).

In vitro and *in vivo* studies clearly underline the two major activities of urolithins: anti-inflammatory and anti-neoplastic (Tomas-Barberan et al., 2016). Additionally, urolithin A was recently shown to improve mitochondrial and muscle function due to the enhancement of mitophagy (Ryu et al., 2016). Nonetheless, low plasma and tissue concentrations of non-conjugated urolithins caused by intensive Phase II metabolism render the activities determined for aglycones *in vitro* inconsistent with *in vivo* data.

DMD Fast Forward. Published on March 10, 2017 as DOI: 10.1124/dmd.117.075200
This article has not been copyedited and formatted. The final version may differ from this version.

Numerous pathological conditions, including inflammatory processes and tumors, are known to be associated with significantly increased levels of extracellular *β*-glucuronidase. Human *β*-glucuronidase is a lysosomal enzyme that accumulates at inflammation sites and in tumor microenvironments due to release from infiltrating neutrophils and macrophages as well as necrotic cells (Tranoy-Opalinski et al., 2014). Mitochondrial respiration defects observed in inflamed and neoplastic tissues lead to aerobic glycolysis—also known as the Warburg effect—resulting in pH decreases due to elevated lactic acid production that creates optimal conditions for *β*-glucuronidase activity (Warburg, 1956a; Warburg, 1956b; Palsson-McDermott and O'Neill, 2013). As a result, autophagy impairment leads to mitochondrial dysfunction that induces *β*-glucuronidase activity (Ishisaka et al., 2013), while damaged mitochondria, similar to bacteria, release formyl peptides that can signal using formyl peptide receptor-1 (FPR1) to trigger an immune response (Sun et al., 2016).

We have clearly shown that urolithin conjugates are cleaved by *β*-glucuronidase, which is released by neutrophils from azurophilic granules upon stimulation of FPR1. The optimum pH, obtained by acidification with lactic acid, was necessary for enzymatic cleavage, as it was not observed in either the environment of pure HBSS or acidified to pH=3.5. Previous studies conducted for luteolin glucuronide have revealed that its deconjugation is triggered by stimulated neutrophils. An increased ratio of aglycone/glucuronide was also observed in the plasma of LPS-treated rats (Shimoi et al., 2001). The *β*-glucuronidase released by macrophages was shown to be essential for activation of quercetin glucuronide conjugates. Its enzymatic activity, which requires acidic pH, was promoted by increased secretion of lactate in response to mitochondrial dysfunction (Kawai, 2014).

DMD Fast Forward. Published on March 10, 2017 as DOI: 10.1124/dmd.117.075200
This article has not been copyedited and formatted. The final version may differ from this version.

The role of selective deconjugation within neoplastic tissues has attracted considerable attention. Since high levels of *β*-glucuronidase can be found in most solid tumors, a wide number of structurally diverse glucuronide prodrugs have been designed with the aim of enhancing the selectivity of cancer chemotherapy.(Tranoy-Opalinski et al., 2014).

Although the highest concentration of urolithin Phase II metabolites were observed in urine, no studies have yet been conducted regarding the impact of these compounds on ailments associated with urinary tract disorders. Uropathogenic *Escherichia coli* (UPEC) is the main cause of urinary tract infections, which produces significant amounts of *β*-glucuronidase (Vinacur et al., 1974; Helander and Dahl, 2005; McLellan and Hunstad, 2016). We have shown that standard strains of *E. coli*, as well as clinical isolates from patients with urinary tract infections, were capable of urolithin glucuronides cleavage. Previous studies conducted for the Phase II metabolites of hydroquinone have shown that *E. coli* cleaved hydroquinone conjugates and liberated toxic free hydroquinone, which is known to possess antibacterial activity (Siegers et al., 2003). To date, no studies regarding the urolithin effects of urinary tract disorders, *E. coli* viability and virulence factors have been conducted. Nevertheless, deconjugation of urolithin glucuronides by *E. coli β*-glucuronidase revealed here indicates the need for examination of both conjugated and non-conjugated urolithins in future studies on the influence of orally administered ET-containing natural products on processes associated with urinary tract infections.

The dominance of urolithins of plasma, tissues and urine glucuronide conjugates is potent, as they release their aglycones directly in inflamed and neoplastic tissues due to enhanced *β*-glucuronidase activity. The release of free aglycones is also possible within urinary tracts infected with *β*-glucuronidase-

DMD Fast Forward. Published on March 10, 2017 as DOI: 10.1124/dmd.117.075200
This article has not been copyedited and formatted. The final version may differ from this version.

producing *E. coli* strains. Strong biological activities, such as the anti-neoplastic and anti-inflammatory activities already described for non-conjugated urolithins (Tomas-Barberan et al., 2016), make intensive detoxification through Phase II metabolism plausible. This process could be responsible for prevention of the impact of urolithins on biochemical processes throughout the entire organism. The conjugation of these pharmacologically active metabolites can be thus seen as a beneficial process, especially considering the formation of these compounds by gut microbiota from ETs that are widely distributed in various food products. It can be hypothesized that the selective activation of urolithin glucuronides by *β*-glucuronidase present at high concentrations at the inflammation site and in the microenvironments of most solid tumors could only locally increase the concentration of bioactive urolithin aglycones. This action can prevent their impact on cellular processes within healthy tissues. To fully support the stated hypothesis, the observed deconjugation should be further confirmed in *in vivo* studies. However, the presented results provide first new insights into understanding urolithin disposition.

Authorship contributions:

Participated in research design: Piwowarski, Stefańska, Kiss

Conducted experiments: Piwowarski, Stanisławska

Contributed new reagents or analytic tools: Granica, Piwowarski

Performed data analysis: Piwowarski

Wrote or contributed to the writing of the manuscript: Piwowarski, Stanisławska

References

Adams LS, Zhang Y, Seeram NP, Heber D, and Chen S (2010) Pomegranate ellagitannin-derived compounds exhibit antiproliferative and antiaromatase activity in breast cancer cells *in vitro*. *Cancer Prev Res (Phila)* 3:108-113.

Chang GW, Brill J, and Lum R (1989) Proportion of beta-D-glucuronidase-negative *Escherichia coli* in human fecal samples. *Appl Environ Microbiol* 55: 335-339.

Dellafiora L, Mena P, Cozzini P, Brighenti F, and Del Rio D (2013) Modelling the possible bioactivity of ellagitannin-derived metabolites. *In silico* tools to evaluate their potential xenoestrogenic behavior. *Food Funct* 4:1442-1451.

Espin JC, Larrosa M, Garcia-Conesa MT, and Tomas-Barberan F (2013) Biological significance of urolithins, the gut microbial ellagic acid-derived metabolites: the evidence so far. *Evid Based Complement Alternat Med* 2013:270418.

Garcia-Villalba R, Espin JC, and Tomas-Barberan FA (2016) Chromatographic and spectroscopic characterization of urolithins for their determination in biological samples after the intake of foods containing ellagitannins and ellagic acid. *J Chromatogr A* 1428:162-175.

Gimenez-Bastida JA, Gonzalez-Sarrias A, Larrosa M, Tomas-Barberan F, Espin JC, and Garcia-Conesa MT (2012) Ellagitannin metabolites, urolithin A glucuronide and its aglycone urolithin A, ameliorate TNF-alpha-induced inflammation and associated molecular markers in human aortic endothelial cells. *Mol Nutr Food Res* 56:784-796.

Gonzalez-Barrio R, Borges G, Mullen W, and Crozier A (2010) Bioavailability of anthocyanins and ellagitannins following consumption of raspberries by healthy humans and subjects with an ileostomy. *J Agric Food Chem* 58:3933-3939.

Gonzalez-Barrio R, Truchado P, Ito H, Espin JC, and Tomas-Barberan FA (2011) UV and MS identification of urolithins and nasutins, the bioavailable metabolites of ellagitannins and ellagic acid in different mammals. *J Agric Food Chem* 59:1152-1162.

Gonzalez-Sarrias A, Espin JC, Tomas-Barberan FA, and Garcia-Conesa MT (2009) Gene expression, cell cycle arrest and MAPK signalling regulation in Caco-2 cells exposed to ellagic acid and its metabolites, urolithins. *Mol Nutr Food Res* 53:686-698.

Gonzalez-Sarrias A, Gimenez-Bastida JA, Garcia-Conesa MT, Gomez-Sanchez MB, Garcia-Talavera NV, Gil-Izquierdo A, Sanchez-Alvarez C, Fontana-Compiano LO, Morga-Egea JP, Pastor-Quirante FA, Martinez-Diaz F, Tomas-Barberan FA, and Espin JC (2010) Occurrence of urolithins, gut microbiota ellagic acid metabolites and proliferation markers expression response in the human prostate gland upon consumption of walnuts and pomegranate juice. *Mol Nutr Food Res* 54:311-322.

Gonzalez-Sarrias A, Gimenez-Bastida JA, Nunez-Sanchez MA, Larrosa M, Garcia-Conesa MT, Tomas-Barberan FA, and Espin JC (2014) Phase-II metabolism limits the antiproliferative activity of urolithins in human colon cancer cells. *Eur J Nutr* 53:853-864.

Gonzalez-Sarrias A, Miguel V, Merino G, Lucas R, Morales JC, Tomas-Barberan F, Alvarez AI, and Espin JC (2013) The gut microbiota ellagic acid-derived metabolite urolithin A and its sulfate conjugate are substrates for the drug efflux transporter breast cancer resistance protein (ABCG2/BCRP). *J Agric Food Chem* 61:4352-4359.

Gonzalez-Sarrias A, Nunez-Sanchez MA, Garcia-Villalba R, Tomas-Barberan FA, and Espin JC (2015) Antiproliferative activity of the ellagic acid-derived gut microbiota isourolithin A and comparison with its urolithin A isomer: the role of cell metabolism. *Eur J Nutr* DOI: 10.1007/s00394-015-1131-7

Gonzalez-Sarrias A, Nunez-Sanchez MA, Tome-Carneiro J, Tomas-Barberan FA, Garcia-Conesa MT, and Espin JC (2016) Comprehensive characterization of the effects of ellagic acid and urolithins on colorectal cancer and key-associated molecular hallmarks: MicroRNA cell specific induction of CDKN1A (p21) as a common mechanism involved. *Mol Nutr Food Res* 60:701-716.

Helander A and Dahl H (2005) Urinary tract infection: a risk factor for false-negative urinary ethyl glucuronide but not ethyl sulfate in the detection of recent alcohol consumption. *Clin Chem* 51:1728-1730.

Ho KJ (1985) Human beta-glucuronidase. Studies on the effects of pH and bile acids in regard to its role in the pathogenesis of cholelithiasis. *Biochim Biophys Acta* 827:197-206.

Ishisaka A, Kawabata K, Miki S, Shiba Y, Minekawa S, Nishikawa T, Mukai R, Terao J, and Kawai Y (2013) Mitochondrial dysfunction leads to deconjugation of quercetin glucuronides in inflammatory macrophages. *PLoS One* 8:e80843.

Kawai Y (2014) beta-Glucuronidase activity and mitochondrial dysfunction: the sites where flavonoid glucuronides act as anti-inflammatory agents. *J Clin Biochem Nutr* 54:145-150.

Kieran T and Del Rio D (2015) *Diet-Microbe Interactions in the Gut. Effects on human health and disease.* Academic Press, London.

Klaassen CD and Cui JY (2015) Review: mechanisms of how the intestinal microbiota alters the effects of drugs and bile acids. *Drug Metab Dispos* 43:1505-1521.

Larrosa M, Garcia-Conesa MT, Espin JC, and Tomas-Barberan FA (2010a) Ellagitannins, ellagic acid and vascular health. *Mol Aspects Med* 31:513-539.

Larrosa M, Gonzalez-Sarrias A, Garcia-Conesa MT, Tomas-Barberan FA, and Espin JC (2006) Urolithins, ellagic acid-derived metabolites produced by human colonic microflora, exhibit estrogenic and antiestrogenic activities. *J Agric Food Chem* 54:1611-1620.

Larrosa M, Gonzalez-Sarrias A, Yanez-Gascon MJ, Selma MV, Azorin-Ortuno M, Toti S, Tomas-Barberan F, Dolara P, and Espin JC (2010b) Anti-inflammatory properties of a pomegranate extract and its metabolite urolithin-A in a colitis rat model and the effect of colon inflammation on phenolic metabolism. *J Nutr Biochem* 21:717-725.

Lucas R, Alcantara D, and Morales JC (2009) A concise synthesis of glucuronide metabolites of urolithin-B, resveratrol, and hydroxytyrosol. *Carbohydr Res* 344:1340-1346.

McLellan LK and Hunstad DA (2016) Urinary Tract Infection: Pathogenesis and Outlook. *Trends Mol Med*.

Mora-Cubillos X, Tulipani S, Garcia-Aloy M, Bullo M, Tinahones FJ, and Andres-Lacueva C (2015) Plasma metabolomic biomarkers of mixed nuts exposure inversely correlate with severity of metabolic syndrome. *Mol Nutr Food Res* 59:2480-2490.

Nunez-Sanchez MA, Garcia-Villalba R, Monedero-Saiz T, Garcia-Talavera NV, Gomez-Sanchez MB, Sanchez-Alvarez C, Garcia-Albert AM, Rodriguez-Gil

FJ, Ruiz-Marin M, Pastor-Quirante FA, Martinez-Diaz F, Yanez-Gascon MJ, Gonzalez-Sarrias A, Tomas-Barberan FA, and Espin JC (2014) Targeted metabolic profiling of pomegranate polyphenols and urolithins in plasma, urine and colon tissues from colorectal cancer patients. *Mol Nutr Food Res* 58:1199-1211.

Palsson-McDermott EM and O'Neill LA (2013) The Warburg effect then and now: from cancer to inflammatory diseases. *Bioessays* 35:965-973.

Pearson AG, Kiefel MJ, Ferro V, and von Itzstein M (2005) Towards the synthesis of aryl glucuronides as potential heparanase probes. An interesting outcome in the glycosidation of glucuronic acid with 4-hydroxycinnamic acid. *Carbohydr Res* 340:2077-2085.

Piwowarski JP, Granica S, and Kiss AK (2014a) Influence of gut microbiota-derived ellagitannins' metabolites urolithins on pro-inflammatory activities of human neutrophils. *Planta Med* 80:887-895.

Piwowarski JP, Granica S, Stefanska J, and Kiss AK (2016) Differences in metabolism of ellagitannins by human gut microbiota *ex vivo* cultures. *J Nat Prod* 79:3022-3030.

Piwowarski JP, Granica S, Zwierzynska M, Stefanska J, Schopohl P, Melzig MF, and Kiss AK (2014b) Role of human gut microbiota metabolism in the anti-inflammatory effect of traditionally used ellagitannin-rich plant materials. *J Ethnopharmacol* 155:801-809.

Piwowarski JP and Kiss AK (2013) C-glucosidic ellagitannins from Lythri herba (European Pharmacopoeia): chromatographic profile and structure determination. *Phytochem Anal* 24:336-348.

Piwowarski JP, Kiss AK, Granica S, and Moeslinger T (2015) Urolithins, gut microbiota-derived metabolites of ellagitannins, inhibit LPS-induced inflammation in RAW 264.7 murine macrophages. *Mol Nutr Food Res* 59:2168-2177.

Ryu D, Mouchiroud L, Andreux PA, Katsyuba E, Moullan N, Nicolet-Dit-Felix AA, Williams EG, Jha P, Lo Sasso G, Huzard D, Aebischer P, Sandi C, Rinsch C, and Auwerx J (2016) Urolithin A induces mitophagy and prolongs lifespan in C. elegans and increases muscle function in rodents. *Nat Med* 22:879-888.

Sala R, Mena P, Savi M, Brighenti F, Crozier A, Miragoli M, Stilli D, and Del Rio D (2015) Urolithins at physiological concentrations affect the levels of pro-inflammatory cytokines and growth factor in cultured cardiac cells in hyperglucidic conditions. *J Funct Foods* 15:97-105.

Seeram NP, Aronson WJ, Zhang Y, Henning SM, Moro A, Lee RP, Sartippour M, Harris DM, Rettig M, Suchard MA, Pantuck AJ, Belldegrun A, and Heber D (2007) Pomegranate ellagitannin-derived metabolites inhibit prostate cancer growth and localize to the mouse prostate gland. *J Agric Food Chem* 55:7732-7737.

Shimoi K, Saka N, Nozawa R, Sato M, Amano I, Nakayama T, and Kinae N (2001) Deglucuronidation of a flavonoid, luteolin monoglucuronide, during inflammation. *Drug Metab Dispos* 29:1521-1524.

Siegers C, Bodinet C, Ali SS, and Siegers CP (2003) Bacterial deconjugation of arbutin by *Escherichia coli*. *Phytomedicine* 10 Suppl 4:58-60.

Sun N, Youle RJ, and Finkel T (2016) The Mitochondrial Basis of Aging. *Mol Cell* 61:654-666.

Tomas-Barberan FA, Garcia-Villalba R, Gonzalez-Sarrias A, Selma MV, and Espin JC (2014) Ellagic acid metabolism by human gut microbiota: consistent observation of three urolithin phenotypes in intervention trials, independent of food source, age, and health status. *J Agric Food Chem* 62:6535-6538.

Tomas-Barberan FA, Gonzalez-Sarrias A, Garcia-Villalba R, Nunez-Sanchez MA, Selma MV, Garcia-Conesa MT, and Espin JC (2016) Urolithins, the rescue of 'old' metabolites to understand a 'new' concept: metabotypes as a nexus between phenolic metabolism, microbiota dysbiosis and host health status. *Mol Nutr Food Res*.

Tranoy-Opalinski I, Legigan T, Barat R, Clarhaut J, Thomas M, Renoux B, and Papot S (2014) beta-Glucuronidase-responsive prodrugs for selective cancer chemotherapy: an update. *Eur J Med Chem* 74:302-313.

van der Hooft JJ, de Vos RC, Mihaleva V, Bino RJ, Ridder L, de Roo N, Jacobs DM, van Duynhoven JP, and Vervoort J (2012) Structural elucidation and quantification of phenolic conjugates present in human urine after tea intake. *Anal Chem* 84:7263-7271.

Vinacur JC, Casellas JM, Rubi RA, and Oneto EP (1974) Serum anti-*Escherichia coli* antibodies and urinary beta-glucuronidase for the diagnosis and control of evolution of urinary infection during pregnancy. *Am J Obstet Gynecol* 120:812-816.

Warburg O (1956a) On respiratory impairment in cancer cells. *Science* 124:269-270.

Warburg O (1956b) On the origin of cancer cells. *Science* 123:309-314.

Yip LY and Chan EC (2015) Investigation of host-gut microbiota modulation of therapeutic outcome. *Drug Metab Dispos* 43:1619-1631.

Footnotes

The project was financially supported by a Polish Ministry of Science and Higher Education research grant, Iuventus Plus [IP2015 062274]. J.P.P. was financially supported by a Foundation for Polish Science START scholarship [START 84.2016]. The project was performed using Centre for Preclinical Research and Technology infrastructure financed by the European Regional Development Fund within the "Innovative Economy" Operational Programme for 2007–2013.

Reprint requests should be directed to:

Dr. Jakub Piwowarski

Department of Pharmacognosy and Molecular Basis of Phytotherapy

Medical University of Warsaw

Faculty of Pharmacy

Banacha 1

02-097 Warsaw

Poland

DMD Fast Forward. Published on March 10, 2017 as DOI: 10.1124/dmd.117.075200
This article has not been copyedited and formatted. The final version may differ from this version.

Legends for Figures:

Fig. 1. Chemical structures of isolated urolithin Phase II metabolites

Fig. 3. ^{1}H NMR spectra of urolithin A-3-*O*-glucuronide and urolithin A-8-*O*-glucuronide mixture (**GUA**).

Fig. 4. (A) Cleavage of GiUA, GUA and GUB by *β*-glucuronidase released by human neutrophils obtained from four donors (D1-D4) and assayed in duplicate. (B) Comparison of release of *β*-glucuronidase protein between f-MLP-stimulated (ST) and non-stimulated (NST) neutrophils. Statistical significance: * $p < 0.05$, ** $p < 0.01$ versus respective non-stimulated controls.

Fig. 5. Chromatograms presenting cleavage of **GiUA**, **GUA** and **GUB** in acidified supernatants (pH= 5.2) obtained from neutrophils isolated from D4 stimulated with f-MLP.

Fig. 6. Cultures of tested *E. coli* standard strains and clinical isolates (C1-C7) in Fluorocult VRB Agar plates visualized with UV light at 366 nm.

Fig. 7. Deglucuronidation of **GiUA**, **GUA** and **GUB** by *β*-glucuronidase released by *E. coli* standard strains and clinical isolates (C1-C7). Three separate experiments were conducted in duplicate. Statistical significance: * $p < 0.05$, ** $p < 0.01$, *** $p < 0.001$ versus other glucuronides within the group. Chromatograms are provided in Supplemental Data Figure S1.

Tables:

Table 1. NMR spectroscopic data (300 MHz, DMSO-d_6) for **GiUA**, **GUA** and **GUB**.

	iso-urolithin A 3-*O*-glucuronide		**urolithin A 8-*O*-glucuronide**		**urolithin A 3-*O*-glucuronide**		**urolithin B 3-*O*-glucuronide**	
	δ_H	δ_C	δ_H	δ_C	δ_H	δ_C	δ_H	δ_C
1	8.12 (d, *J*=8.9 Hz)	125.14	8.09 (d, *J*=8.9 Hz)	124.37	8.15 (d, *J*=9.1 Hz)	123.67	8.17(o)	125.14
2	7.05 (o)	113.83	6.83 (dd, *J*=8.7, 2.4 Hz)	113.16	7.03 (dd, *J*=8.8, 2.5 Hz)	113.64	7.04 (dd, *J*=8.6, 2.1 Hz)	114.24
3		159.05	10.24 (s) (OH)	159.20		157.39		158.79
4	7.07 (o)	104.29	6.75 (d, *J*=2.4 Hz)	102.89	7.08 (d, *J*=2.4 Hz)	103.86	7.03 (s)	104.24
4a		152.57		151.37		150.55		151.96
6		160.61		160.35		160.39		161.24
6a		112.42		120.08		120.77		119.58
7	8.08 (d, *J*=8.7 Hz)	132.97	7.74 (d, *J*=2.7 Hz)	114.90	7.54 (d, *J*=2.6 Hz)	113.64	8.15(o)	130.16
8	7.02 (o)	117.60		156.15	10.31 (s) (OH)	157.54	7.58 (t, *J*=7.7 Hz)	129.05
9		164.30	7.56 (dd, *J*=8.6, 2.7 Hz)	124.95	7.34 (dd, *J*=8.7, 2.7 Hz)	124.10	7.87 (t, *J*=7.7 Hz)	136.10
10	7.53 (d, *J*=2.1 Hz)	107.23	8.23 (d, *J*=9.0 Hz)	123.64	8.18 (d, *J*=9.1 Hz)	123.76	8.21 (d, *J*=8.9 Hz)	122.39
10a		137.28		129.77		126.26		134.70
10b		111.52		109.36		112.46		112.46
Glur1	5.23 (d, *J*=7.2 Hz)	99.97	5.22 (d, *J*=7.2 Hz)	100.25	5.21 (d, *J*=7.3 Hz)	99.60	5.15 (d, *J*=6.8 Hz)	99.88
Glur2	3.32(o)	73.32	3.30-3.45 (o)	72.99	3.30-3.45 (o)	72.87	3.34 (o)	73.14
Glur3	3.35(o)	76.18	3.30-3.45 (o)	75.74	3.30-3.45 (o)	75.54	3.38 (o)	75.88
Glur4	3.42(o)	71.76	3.30-3.45 (o)	71.32	3.30-3.45 (o)	71.29	3.40 (o)	71.69
Glur5	4.03 (d, *J*=9.2 Hz)	75.79	3.99 (d, *J*=9.2Hz)	75.46	4.02 (d, *J*=9.2 Hz)	75.34	4.02 (d, *J*=9.2 Hz)	75.56
Glur6		170.56		170.05		170.08		170.71

s- singlet, d- doublet, dd- doublet of doublets, t- triplet, o- overlapped signals

Figures

Figure 1

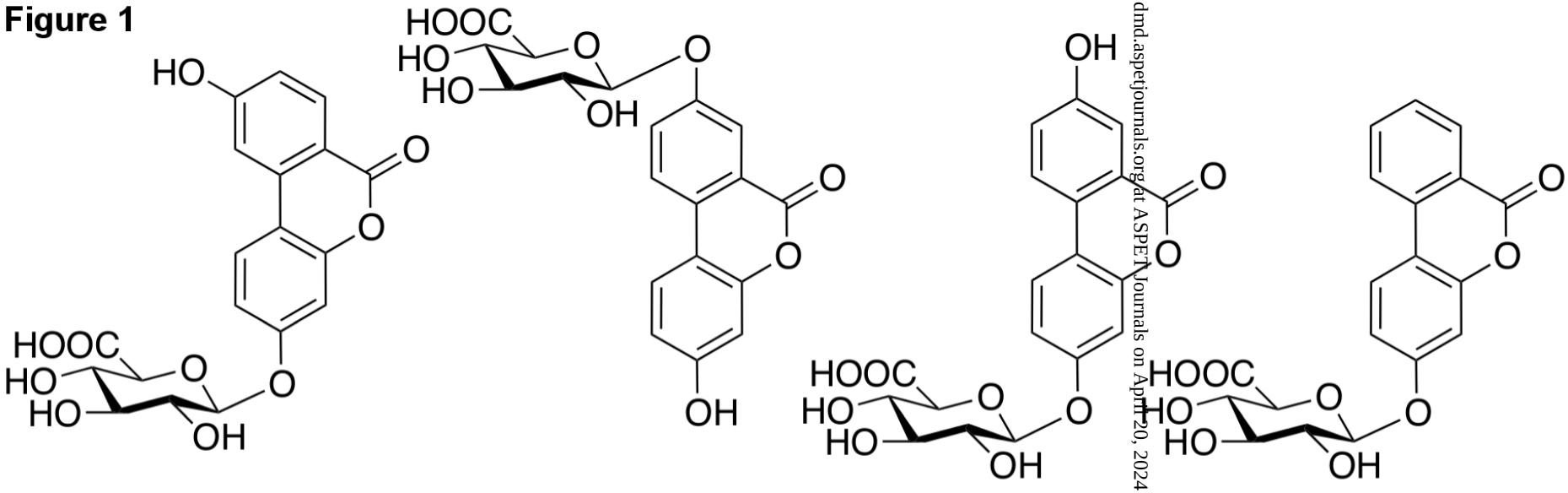

Figure 2

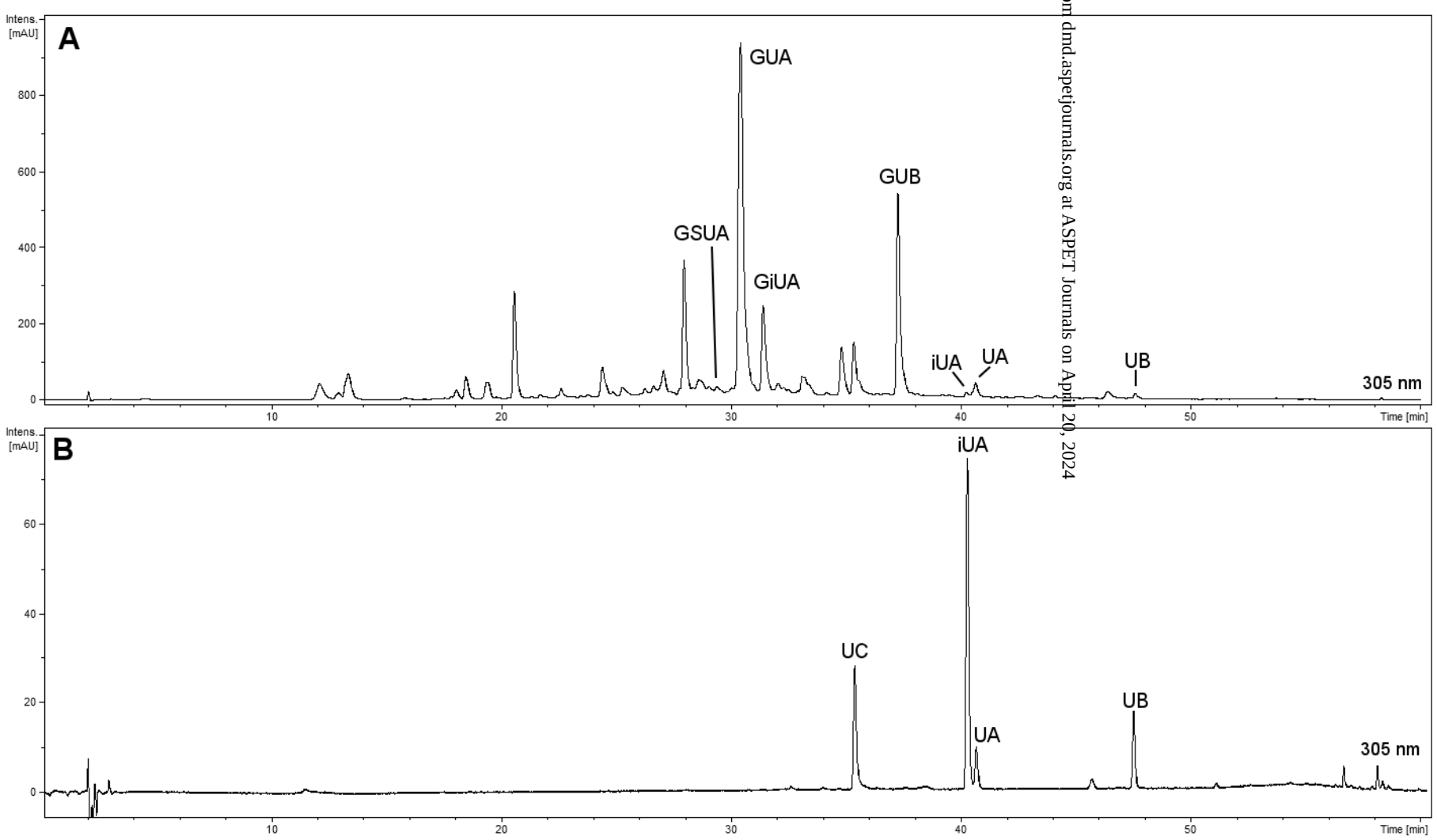

Figure 3

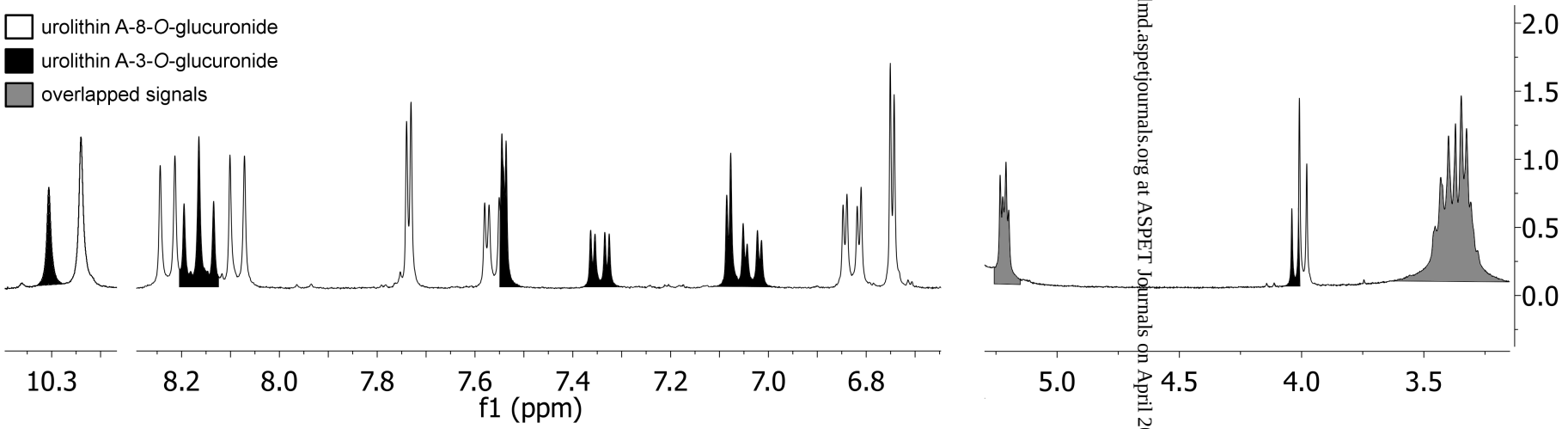

DMD Fast Forward. Published on March 10, 2017 as DOI: 10.1124/dmd.117.075200
This article has not been copyedited and formatted. The final version may differ from this version.

Figure 4

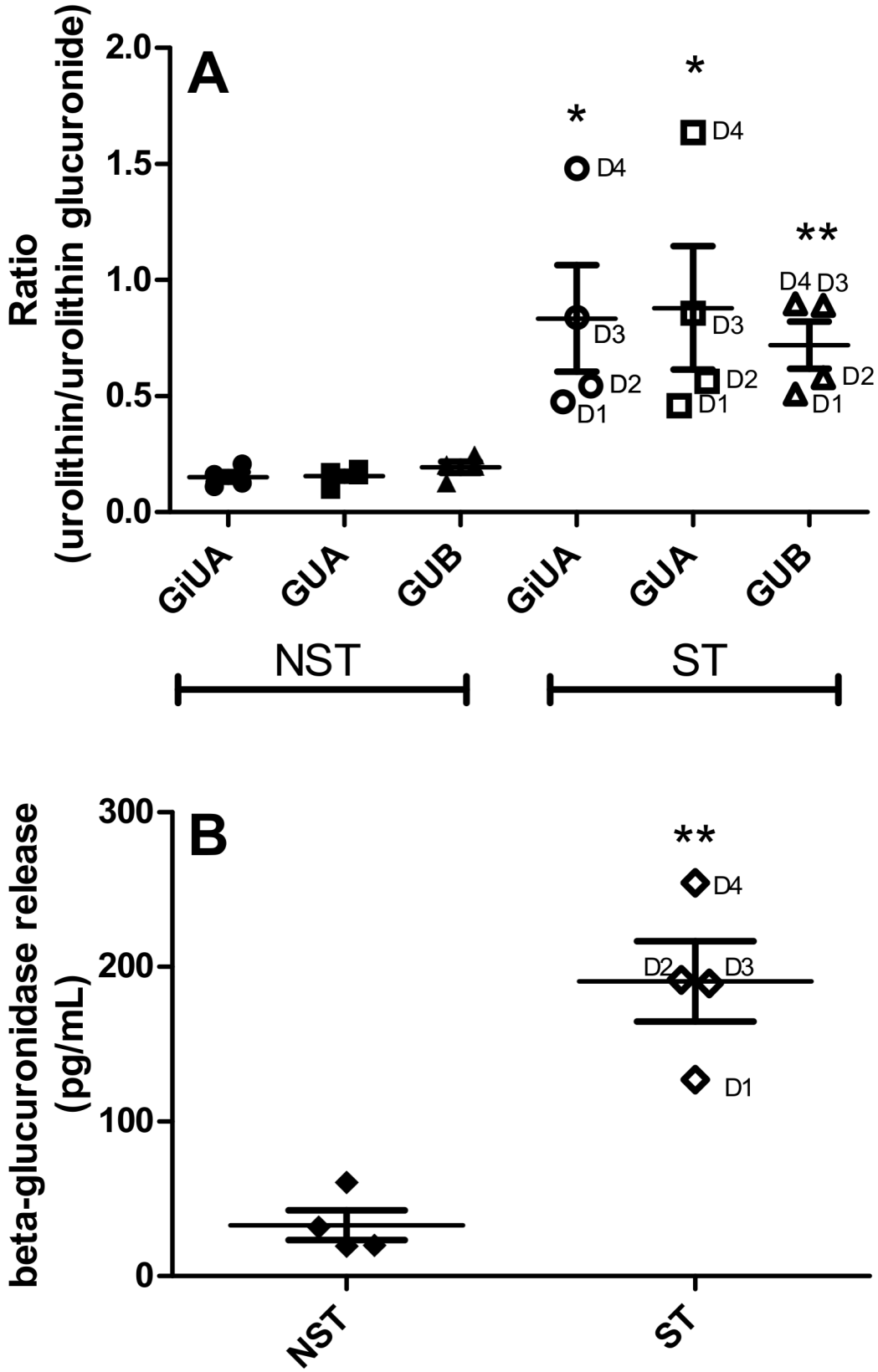

DMD Fast Forward. Published on March 10, 2017 as DOI: 10.1124/dmd.117.075200
This article has not been copyedited and formatted. The final version may differ from this version.

Figure 5

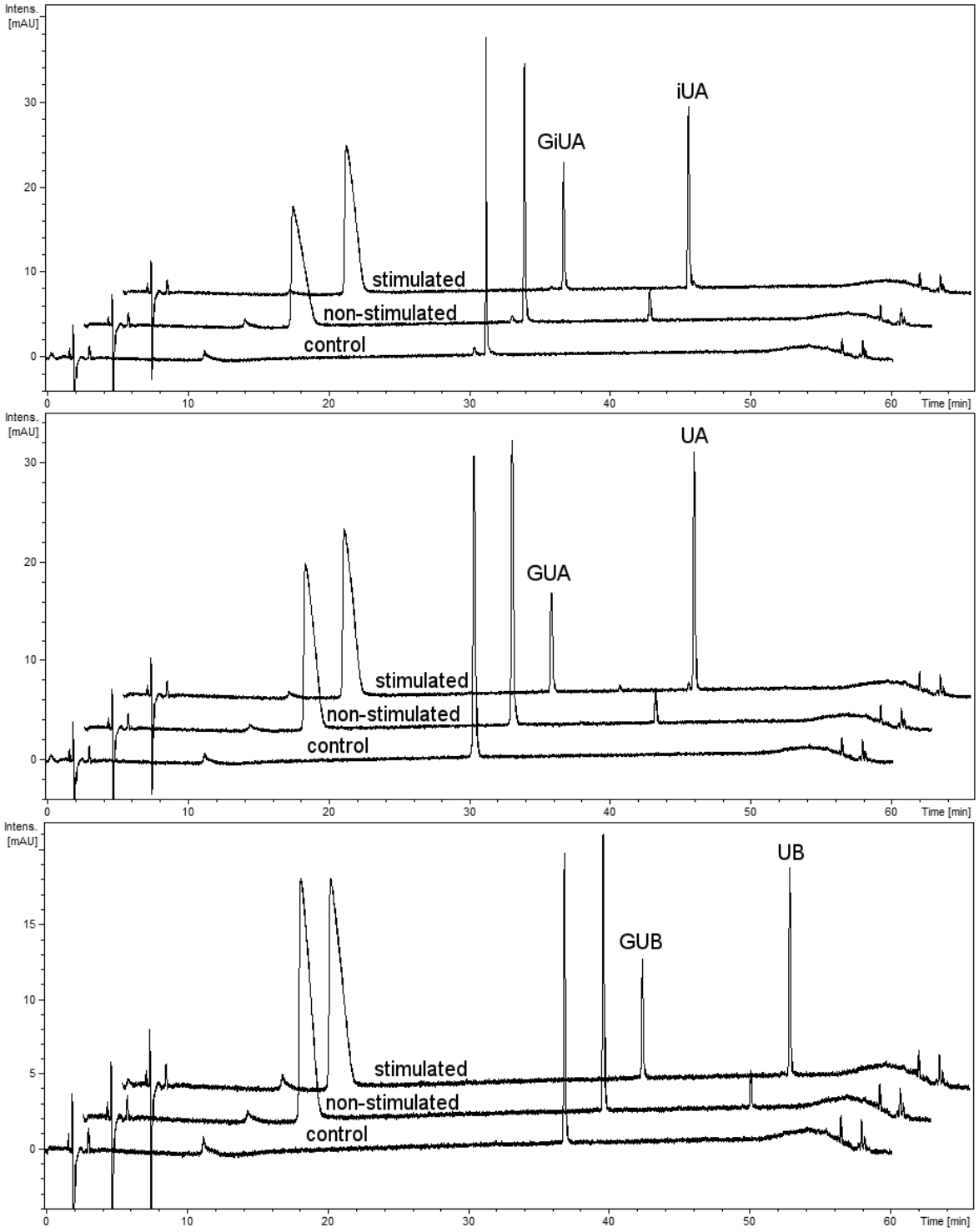

DMD Fast Forward. Published on March 10, 2017 as DOI: 10.1124/dmd.117.075200
This article has not been copyedited and formatted. The final version may differ from this version.

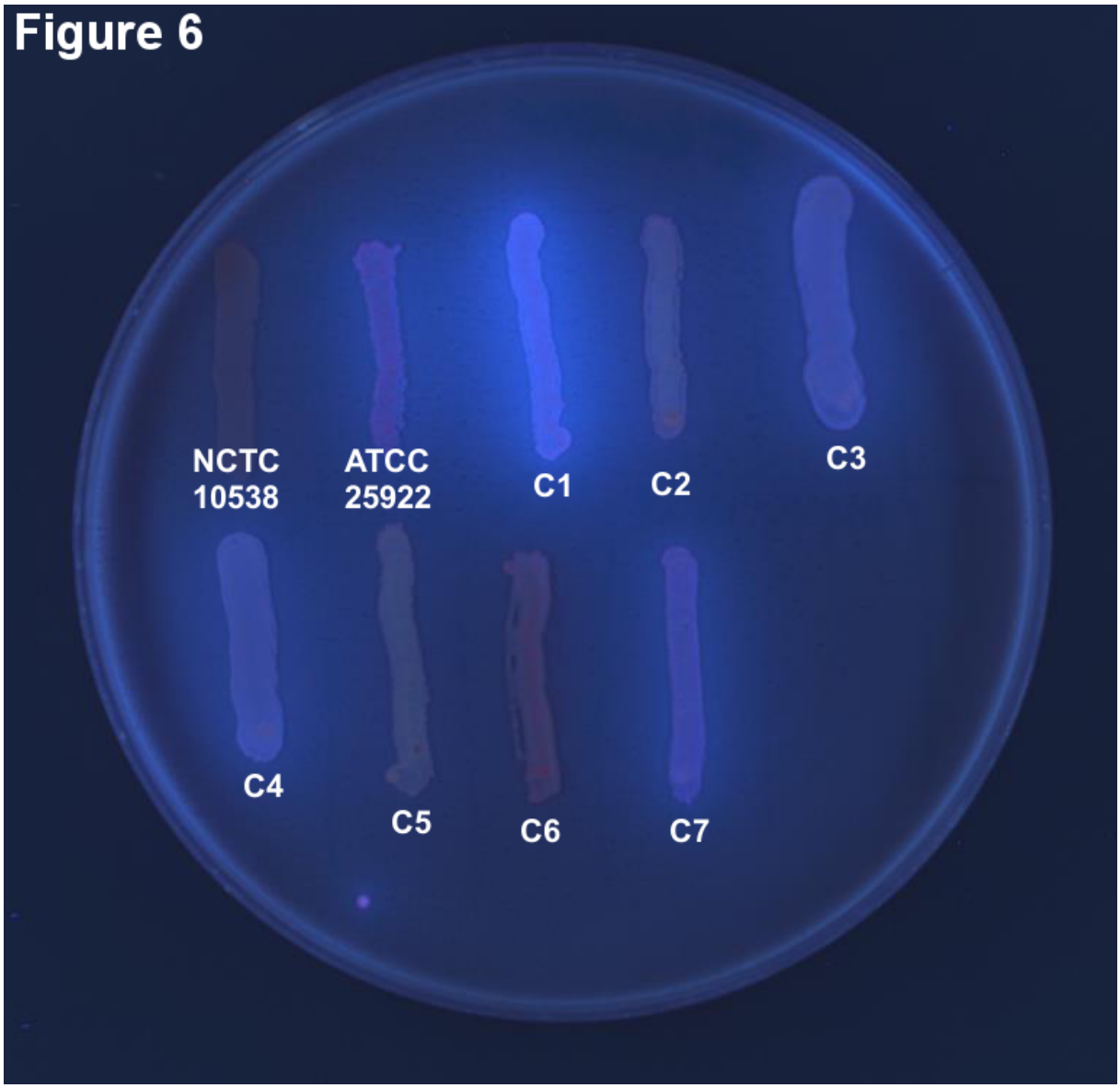

Figure 7